

# Flow Transients of Vacuum Ejector Operation with Straight Cylindrical Primary Duct

Dr.SLN.Desikan <sup>\*1</sup>, Arun.A. K<sup>#2</sup>, N.Sankareswaran <sup>\*\*3</sup>

<sup>\*</sup>Scientist, Vikram Sarabhai Space Centre, Thiruvananthapuram

<sup>#</sup>Assistant Professor & Aeronautical Engineering, PSN College of Engineering and Technology, Tirunelveli

<sup>\*\*</sup>Assistant Professor & Mechanical Engineering, Anna University Regional campus, Tirunelveli

## Abstract

A detailed understanding of a flow analysis through a vacuum ejector is necessary to improve the performance of vacuum ejector. For each vacuum ejector geometry, there will be a particular primary jet pressure window in which minimum secondary vacuum can be achieved. The objective of this study is to understand the transient flow behaviour through a simple vacuum ejector model in which the flow expands from cylindrical primary duct into one side closed ducts namely rectangular duct and divergent duct and to compare the vacuum ejector performance by changing the height of secondary chamber of these two ducts for different operating pressures ranging from 2 bar to 5 bar.

**Keywords** - vacuum ejector, Flow transients, vacuum generation, flow ejector

## I. INTRODUCTION

An ejector is a simple device consisting of no moving parts, lubricants or seals, used for transporting or inducing a low-pressure secondary fluid by using a high-pressure, high-velocity primary fluid flow due to the shear action generated by the primary jet. An ejector consists of a supersonic propulsive primary nozzle, a passive secondary nozzle, mixing throat and a supersonic exhaust diffuser.

Ejectors are extensively used in power plants, chemical industries and refineries, aerospace application etc for the thrust augmentation of V/STOL, high-altitude simulation facility, combustion facility, refrigeration system, natural gas generation, fuel cells, noise-control facility, desalination plants, vacuum degassing devices, jet pumps, wind tunnel etc. due to the advantage that it can compress and transport a large amount of fluid with a small driving energy (energy saving device), it's little maintenance, it's lenience and reliability with low capital and maintenance costs.

Depending on the function of ejector system, it can be classified into three such as a compressor, a fluid transport device and a vacuum pump. In a compressor system, it compresses the secondary low-pressure stream in the mixing chamber by using high-pressure primary stream. In a fluid transportation device, the ejector will drag and carry the secondary stream along with the primary stream. In a vacuum

pump, high-vacuum levels in the secondary chamber is created which is required in high altitude testing (HAT) simulations by dragging mass flow from a finite secondary chamber.

Depending on the position of nozzle, ejectors can be classified as constant pressure and constant area ejectors. Based on type of fluid used- water ejectors, steam ejectors, gas ejectors and air ejectors.

The diffuser inlet of a vacuum ejector experiences a low pressure due to the expansion of primary jet which will be less than secondary chamber pressure. Due to this pressure difference along with the turbulent entrainment through the shear layer provides the driving force for the secondary stream induction. Ejector systems are commonly used in situations where high pressure stream is already available and that associated flow energy can be utilized to mix and transport fluids by designing suitable aerodynamic passages.

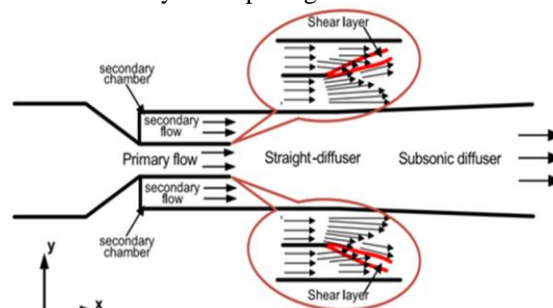


Fig 1.1: Schematic of Vacuum Ejector-Diffuser System

Testing of upper-stage rocket motors with high area ratio nozzles is quite challenging due to a multitude of complexities. For instance, under the vacuum ambient condition of an upper-stage motor, ignition may be improper, some structural components may fail due to out-gassing, and the thrust tail off transient may not proceed as expected. These problems cannot be identified in a sea-level test. When the nozzle back pressure is not sufficiently low, flow separation may occur, thus giving a lower thrust value in a static test. To alleviate these difficulties and to qualify the upper stage motors, it is essential to simulate high-vacuum conditions in a high-altitude test facility. In a HAT facility, the exhaust from the rocket motor is pumped out by a suitable fluid dynamic system, which also aids in gradual pressure recovery from vacuum to atmospheric pressure.

## II. AUTO DESK INVENTOR SOFTWARE

Autodesk inventor is developed by U.S. based software company Autodesk, is a computer-aided design application for mechanical design, simulation, visualization, and documentation. With inventor software, engineering can 2D and 3D data into a signal design environment, creating a virtual representation of the final product that enables them to validate the form, fit and function of the product before its ever built. Autodesk inventor includes power parametric, direct edit and freedom modelling. Autodesk inventor competes directly with solid works, solid edge and CREO.

In case of especially mechanical part design development of the software many industrial can be follow that special characteristic of software an additional module named the aerospace sheet metal design offers the user combine the capabilities of generative sheet metal design and generative surface design. INVENTOR offers a solution to shape design, styling, surfacing workflow and visualization to create, modify and validate complex innovative shapes from industrial design. INVENTOR supports multiple stages of product design whether started from scratch or from 2D sketches

The different tools used in inventor software are

- Operation
- Profile
- Edit sketch
- Extrude mode
- Constrain

## III. SCHILEREN FLOW VISUALIZATION TECHNIQUE

The schlieren flow visualization techniques, which translate phase speed differences in light, invisible to the eye, into changes in intensity which we perceive as regions of light and dark. Change in phase speed as light passes through a transparent medium is called refraction. The refractive index  $n = C_0/C$  of a medium describes the change in phase speed where  $C$  is the speed of light in the medium and  $C_0$  is the speed of light in a vacuum. For gases the refractive index is linearly dependent on the gas density according to the Gladstone-Dale relation:

$$n = K\rho + 1$$

We see that ray deflection is dependent not only on the refractive index of the medium but mainly on the gradients in  $n$  orthogonal to the ray propagation direction. Because of the integral in  $z$ , deflection is also quite sensitive to the extent of the region of varying density in the  $z$ -direction. These deflections are what are made visible by schlieren techniques.

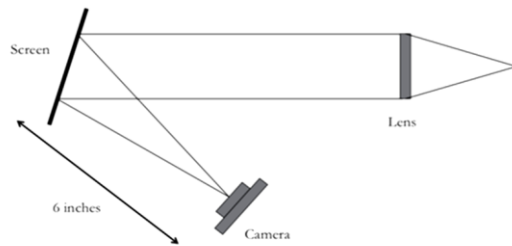


Fig 2: To-Scale Recommended Layout for the Schlieren System.

## IV. PARTICLE IMAGE VELOCIMETRY

PIV is a non-intrusive method of flow visualization, it works via the illumination of particles suspended in the fluid, and these particles follow the fluid flow and as such can be used to study the properties of the flow such as its structure. PIV does not track each particle individually, that is a similar but separate technique known as Particle Tracking Velocimetry (PTV), and rather the bulk movement of particles within an interrogation area is tracked. Evaluation of image acquisition is based on the elemental equation where the distance expresses shift traces particles entrained in the fluid stream at a time.

Therefore, desired position of particles can be record as accurately as possible. It is important that the position of the particles did not change during the illumination. That is, the light has to be short, therefore, the laser light is continuous, but the laser sends pulses. It is necessary to record two records the position of the particle. First record captures the initial position of the particle and the second recording captures its end position. There are two methods and to record the individual exposure method and doubled exposure method.

### A. Analysis of PIV Image

The recorded images are divided into smaller areas evaluation which is square shape. The analysis deals with the investigation of the average displacement of particles in each of the evaluation area. The relationship between the dimensions of the investigated area in object and image plane magnification  $M$ .  $M = \text{object} / \text{image}$

$$\Delta x = \Delta X / M, \Delta y = \Delta Y / M$$

Where  $\Delta x$  and  $\Delta y$  are the displacements in object plane and  $\Delta X, \Delta Y$  are the displacements in the image plane. Each particle has an associated velocity vector  $w_x, w_y$ .

$$w_x = \Delta x / \Delta t, w_y = \Delta y / \Delta t$$

To evaluate the average displacement of the particles has an effect saturation flow. Poor saturation - can be expected with high probability that the evaluation range is not more than 1 part. When using double exposure will be in two images - start and end position of the particle. The determination of the average displacement in this case is simple, but in practice, this saturation unsuitable because of the fact that in certain areas, evaluation may occur more

particles and some particles may be completely missing. And then the information about the speed field is incomplete.

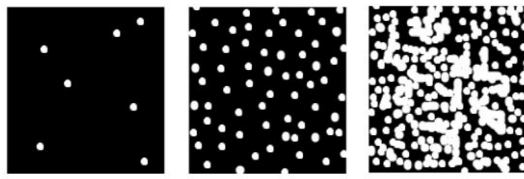


Fig 3: Types of Flow Saturation

### B. CCD camera

Recording PIV images can be recorded position of the reference particle CCD camera or camera. It is currently used to record the particular CCD camera used at intervals of less than one microsecond will record and store the two images together. These Data provide important information on the evolution of current to be measured over time. The screen display can be animated to follow the temporal evolution of the vector field. Maximum image resolution is 2048x2048 pixels.

### C. Laser

The basis of the captured reference particles is those of the light intensity of the plane and thus the light energy in the measurement plane to be large enough for the light intensity distribution on the reference particles was sufficient for the camera preview camera optionally no optical noise. The length of light pulse should be so short that illuminated tracer particles undergone least possible distance. The time interval of consecutive light pulses must be as short reference to the movement of particles in the flow field was very small. Thus, the maximum displacement of the reference particles in divided areas of evaluation, to be measured for the level distribution is less than a quarter of the area being evaluated. The laser: 15 Hz with pulse energy 65-200mJ, compact, lightweight, stable. The cooling system allows long-term use of the laser. Working with laser is dangerous because most frequently used YAG laser emits infrared light with a wavelength of 1064nm especially for vision, therefore it is necessary to wear protective clothing, namely: jacket, glasses.

### D. Setup

Light scattering particles are added to the flow. A laser beam is formed into a light sheet illuminating seeding particles twice with a short time interval  $\Delta t$ . The scattered light is recorded onto two consecutive frames of a high-resolution digital camera. Microscopic, endoscopic and macroscopic configurations cover a wide range of applications in gaseous and liquid media.

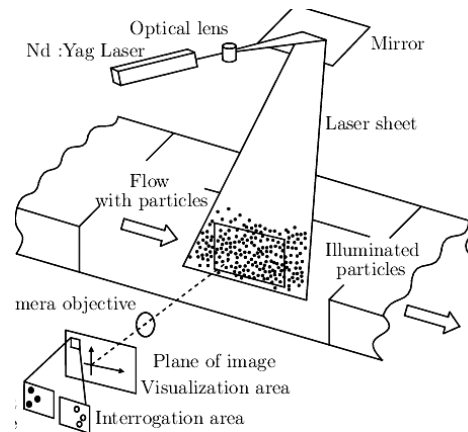


Fig 4: Setup for PIV

### E. Evaluation

The particle image is subdivided into small interrogation windows. For each interrogation window the average particle image separation ( $\Delta x$ ,  $\Delta y$ ) is determined by cross correlation and localization of the correlation peak. When  $M$  is the magnification of the camera the velocity components ( $u$ ,  $v$ ) in this interrogation window is given by  $u = (1/M) (\Delta x/\Delta t)$  and  $v = (1/M) (\Delta y/\Delta t)$

### F. Spatial and temporal derivatives

From one velocity field a range of spatial derivatives can be calculated such as vorticity and shear stress. Ensemble statistics provide additional information like turbulent kinetic energy or Reynolds stresses. Time-resolved velocity fields recorded with high-frame-rate cameras and high frequency laser allow for deeper dynamic insights about flow field evolution, fluid element trajectories, acceleration and turbulence statistics.

## V. METHODOLOGY

### A. Experimental Set Up

The Fig 6.1 shows an experimental set up for analysing the flow transients through a vacuum ejector model. It consists of mainly settling chamber, straight cylindrical primary duct, closed secondary chamber (vacuum chamber), and diffuser/mixing section. The vacuum chamber and diffuser section will vary according to different experimental cases as constant area and divergent duct. A high-pressure air is supplied to the cylindrical primary duct by using air breathing rig (ABR) facility available at wind tunnel data division, VSSC, Trivandrum as shown in Fig.6.2. The ratio of secondary chamber height ( $H_s$ ) to the primary duct exit height ( $D_p$ ) for this geometry varies as 3.25, 2.75, and 2.25 for different experimental cases. The schematic diagram of constant area vacuum ejector and divergent vacuum ejector for this experiment is shown in Fig 6.3 and 6.4 respectively.



Fig 5: Vacuum Ejector - Diffuser Experimental Set Up

This model is started by suddenly opening the primary jet valve in the ABR facility to the required settling chamber pressure and allowing the primary jet to expand into the diffuser section. During start-up, when the primary jet is choked at the primary duct exit, an under expanded jet will be produced in the diffuser section. By changing primary jet total pressures and height of diffuser and secondary chamber of above two configurations, experiments have been conducted for investigating the effect of geometry on vacuum generation.

The flow transients in the vacuum chamber and diffuser section can be visualized by using a time resolved Schlieren technique during the primary jet total pressure ramping process. The different operating conditions (test plan) for this vacuum ejector flow analysis are described on Table below. The pressure variations in the vacuum chamber and in the diffuser, section can be measured by using Endevco 21 P1Y (0- 3bar (absolute)) series piezo-resistive transmitter and the primary jet settling chamber pressure is measured by using Endevco PAA 21Y (0-10 bar (absolute)) series piezo-resistive transmitter.

Table 1: Order of Test Planned

Test no 1		
Components	Length	Height
primary duct	120	40
secondary chamber	120	130
Diffuser	250	150
Test no 2		
Components	Length	Height
primary duct	120	40
secondary chamber	120	110
Diffuser	250	130
Test no 3		
Components	Length	Height
primary duct	120	40
secondary chamber	120	90
Diffuser	250	110

## VI. SUMMARY OF TEST PLAN

A total of 42 number of tests is required to complete this test without including repeatability of tests - [(3 number of tests by changing secondary chamber height for divergent diffuser + 3 number of tests by changing secondary chamber height for straight diffuser)] 7 number of tests by changing operating pressure.

### A. Test conditions

Inputs:

- Total pressure ranging from 2 - 5 bar
- Stagnation temperature 300 K

Outputs:

- Time resolved Schlieren flow visualization. (High speed imaging)
- Unsteady pressure measurements on secondary chamber and diffuser sections.
- Stagnation pressure measurements on settling chamber.
- Synchronized Schlieren images with respect to tunnel stagnation pressure

### B. Design Calculations

For a given inlet stagnant pressure P and temperature T, the mass flow through the cylindrical primary duct at choking condition follows the gas dynamic equation as below.

$$\dot{m} = \frac{P \cdot A_t}{\sqrt{T}} \times \sqrt{\frac{\gamma}{R} \left( \frac{2}{\gamma + 1} \right)^{\frac{\gamma + 1}{\gamma - 1}}}$$

Table 2: Run Time Calculation

TOTAL PRESSURE (N/m <sup>2</sup> )	TOTAL DENSITY (kg/m <sup>3</sup> )	MASS FLOW RATE (kg/S)	RUN TIME (S)
200000	2.32288	0.5867	166.28
250000	2.90360	0.7333	121.94
300000	3.48432	0.8800	92.379
350000	4.06504	1.0267	71.264
400000	4.64576	1.1734	55.427
450000	5.22648	1.3201	43.110
500000	5.80720	1.4667	33.256
550000	6.38792	1.6134	25.194
600000	6.96864	1.7601	18.475
650000	7.54936	1.9068	12.790



### G. Calculation of Thickness of Parts

When air is flowing over the surface of a flat plate, the maximum stress acting on it when its short edge fixed, can be determined by the formula

$$\sigma_b = \frac{0.75b^2p}{h^2 \left(1 + 0.8 \frac{b^4}{a^4}\right)}$$

hoops stress acting on cylindrical primary duct when air is flowing through it, can be calculated by the formula

$$\sigma = PD_m/2t$$

Hence thickness of cylindrical duct can be calculated by the formula

$$t = \frac{PD_i}{2\sigma - P}$$

Since the primary aim of this project is to measure maximum vacuum which has generated inside the secondary chamber, it is necessary to ensure that there is no leakage of air or air entering inside. Thus vacuum ejector should design very carefully in order to avoid leakage of air. Each part of design should be fabricated very accurately and should be connected properly to avoid leakages. The room temperature vulcanizing silicone sealant had used for sealing the components and gasket is used between the faces of parts to be connected to make leakproof.

## VII. MODELLING OF VACUUM EJECTOR-DIFFUSER SYSTEM

Model is a representation of an object, a system, or an idea in some form other than that of the entity itself. Modelling is the process of producing a model, a model is a representation of the construction and working of some system of interest. A model is similar to but simpler than the system it represents. One purpose of a model is to enable the analyst to predict the effect of changes to the system. On the one hand, a model should be a close approximation to the real system and incorporate most of its salient features. On the other hand, it should not be so complex that it is impossible to understand and experiment with it. A good model is a judicious trade-off between realism and simplicity. In this project, modelled a vacuum ejector diffuser system as shown in Fig 6 This assembly system mainly consists of a cylindrical primary duct, a closed vacuum chamber and a divergent diffuser section. The assembly shown in Fig 6 has made up of using 7 parts namely flange, connecting pipe, closing plate, rectangular box, cylindrical primary duct, tapered plate and glass side cover.

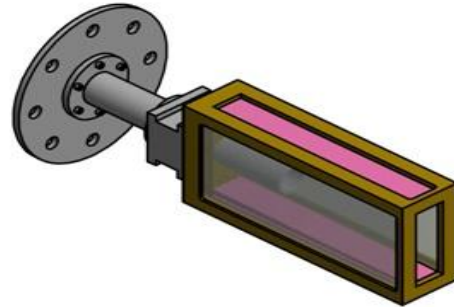


Fig 6: Vacuum Ejector- Divergent Diffuser System

It is very difficult to design vacuum ejector diffuser model which satisfies all different cases in single model itself due to the limitation of minimizing complete leakage of air and due to brittle characteristics of glass. Finally, a single model which satisfies all experimental cases has been modelled by compromising with the wastage of material in machining process and consuming more time to machine the components with very great care and accuracy. This model has an advantage that it needs only one set of float glass to conduct all experimental cases. It is possible to conduct different experiments by changing the appropriate parts and screwing it on the point where the current ejector geometry dimension's needed.

These two different models can be assembled by using the same 9 parts. A total of 3 tests are planned for conducting different experimental case for one ejector model to analyse the effect of secondary chamber volume on vacuum ejector performance. Similarly, for divergent models, it needs a total of 3 tests. The location of pressure sensor on model is also planned and a total of 3 pressure probe has to be located on the model.

### H. Fabrication

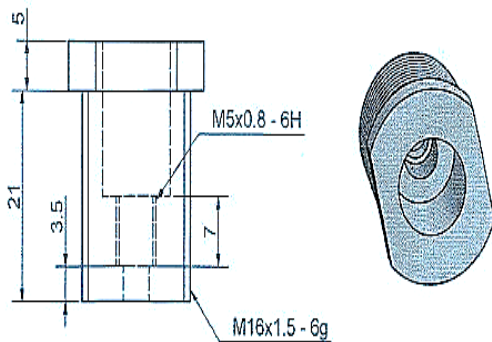
The fabricated model of vacuum ejector diffuser system is shown below. By using lathe machines, milling machines and drilling machines available at SWTD workshop in VSSC, the different components had fabricated. The machining operations like facing, turning, drilling, threading and end milling had done to get this model. To make a slot inside the part to fix the float glass, woodruff cutting tool is used for removing material.



Fig 7: Assembly of Vacuum Ejector - Diffuser Model

**I. Endevco Adaptor**

Since the same one side tapered plate is used for conducting different experimental cases for constant area vacuum ejector model and divergent vacuum ejector model, it is not possible to locate unsteady pressure sensors on the plate which is equal to same distance from the reference point. Hence, an endevco adaptor had modelled by using inventor software for mounting the unsteady pressure sensor on secondary chamber and diffuser sections for both constant area vacuum ejector model and divergent vacuum ejector model. By this design, it is possible to mount unsteady pressure sensors on the plate for different experimental cases. Instead of mounting unsteady pressure sensors directly on the plate, if mounting the unsteady pressure sensors inside the endevco adaptor, it is possible to measure unsteady pressure at same point for different vacuum ejector models and this endevco adaptor with unsteady pressure sensor will be mounted to the plate to measure unsteady pressure on that point. Three endevco adaptor had fabricated for measuring unsteady pressures on three different points of each model.



**Fig 8: Endevco Adaptor – Front view**

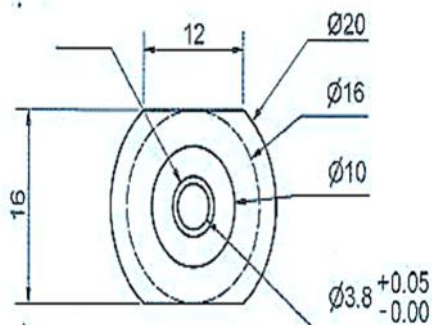


**Fig 9: Endevco Adaptor – Top view**

**J. Schlieren Flow Visualization Arrangement**

The Schlieren flow visualization system has been arranged for this model to know how the flow evolution takes place inside the model and to know the movement of shock inside it. Z- type Schlieren arrangement has done for this model which is shown in Fig

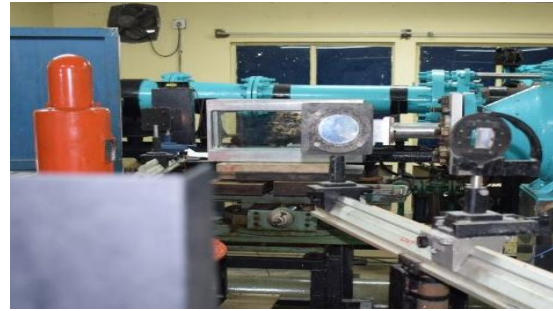


**Fig 10: Schlieren Flow Visualization Arrangement**

**K. Particle Image Velocimetry Arrangement**

The Assembled Model with PIV System Is Shown in Figure

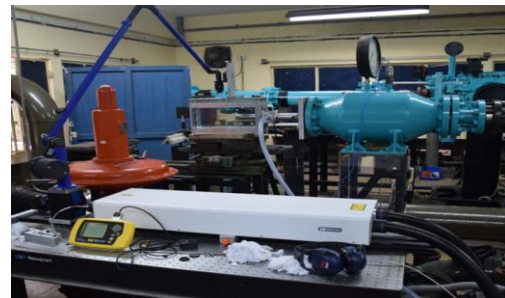


**Fig 10: PIV System Arrangement with Model**

**VIII. RESULTS AND DISCUSSION**

The flow evolution through the model is shown below.

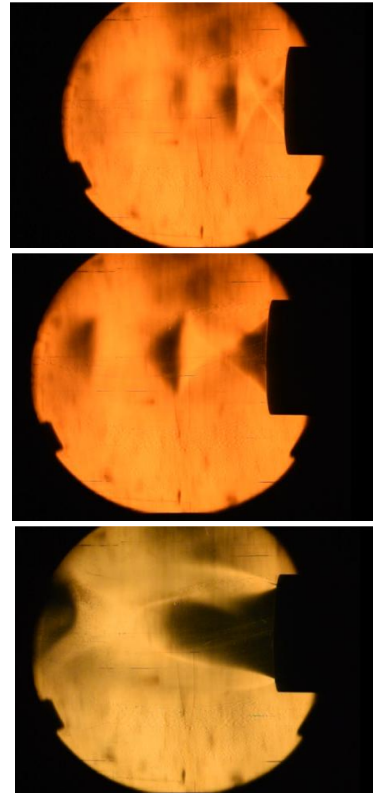


**Fig 11: Flow Evolution in the Model at 5 Bar Pressure**

When high pressure air supplied to the cylindrical primary duct reaches its ends, from the Schlieren image, it is understood that an under expansion occurs in the model and a shock train is formed inside the model.



Fig 12: Shock Train Formed inside the Model

MPG Comparison with and without HHO It was concluded that the car experienced an increase of 4.86 miles per gallon combined (highway and city), going from 19.42 to 24.27 mpg. This is a 25% decrease of fuel consumption, which is an astonishing amount. This shows proof that HHO gas, as an additive to a car, does work and saves the consumer money on their gas expenditure.

## IX. CONCLUSION

For each vacuum ejector geometry, there will be a particular primary jet pressure window in which minimum secondary vacuum can be achieved. Hence in this project, there will be two different vacuum ejector-diffuser configurations namely divergent and constant- area diffuser models. For each vacuum ejector diffuser models, the unsteady pressure at top secondary chamber, bottom secondary chamber and bottom diffuser will be measured by using unsteady pressure sensors located on the corresponding locations. By comparing the results obtained from pressure sensors on these two different vacuum ejector configurations, analyze which ejector has created more vacuum in vacuum chamber. For each vacuum ejector models, the flow transients through the model will be thoroughly studied by analyzing the results obtained from schlieren flow visualization technique.

## REFERENCES

- [1] 2 A. L. Addy, J. C. Dutton, and C. D. Mikkelsen, "Supersonic Ejector-Diffuser Theory and Experiment," Report No. ADP000536, University of Illinois, Urbana, 1981.
- [2] 3 A. Mittal, G. Rajesh, V. Lijo, and H. D. Kim, "Starting transients in vacuum ejector-diffuser system," J. Propul. Power 30(5), 1213–1223 (2014).
- [3] 4 Arun kumar and G.Rajesh , "Flow transients of vacuum ejector at started and un-started mode operation", 2016.
- [4] 5 B. H. Park, J. H. Lee, and W. Yoon, "Studies on the starting transient of a straight cylindrical supersonic exhaust diffuser: Effects of diffuser length and pre-evacuation state," Int. J. Heat Fluid Flow 29(5), 1369–1379 (2008).
- [5] 6 B. H. Park, J. H. Lim, and W. Yoon, "Fluid dynamics in starting and terminating transients of zero-secondary flow ejector," Int. J. Heat Fluid Flow 29(1), 327–339 (2008).
- [6] 7 B. J. Huang, C. B. Jiang, and F. L. Hu, "Ejector performance characteristics and design analysis of jet refrigeration system," Trans. ASME: J. Fluids Eng. 107, 792–802 (1985).
- [7] 8 B. J. Huang, J. M. Chang, C. P. Wang, and V. A. Petrenko, "A 1-D analysis of ejector performance," Int. J. Refrig. 22, 354–364 (1999).
- [8] 9 B. Mandell, B. L. Mc Farland, R. E. Nelson, and G. O. Patmor, "Scale model testing of 90 deg Supersonic turn ejector systems for altitude simulation," J. Spacecr. Rockets 1(1), 108–111 (1964).
- [9] 10 Bruce ralphin rose, Veni grace, "An computational analysis of lobed nozzle ejectors for high altitude simulation of rocket engines", 2014.
- [10] 11 C. J. Wojciechowski and P. G. Anderson, "Parametric analysis of diffuser requirements for high expansion ratio space engine," NASA Technical Note LMSC-11REC TR D784489, 1981.
- [11] 12 D. Drikakis, "Bifurcation phenomena in incompressible sudden expansion flows," Phys. Fluids 9(1), 76–87 (1997).
- [12] 13 D. E. Paxson and K. T. Dougherty, "Ejector enhanced pulsejet based pressure gain combustors: An old idea with a new twist," 41st Joint Propulsion Conference and Exhibit, Arizona, USA, 10–13 July 2005.
- [13] 14 F. Durst, J. C. F. Pereirat, and C. Tropea, "The plane symmetric sudden-expansion flow at low Reynolds numbers," J. Fluid Mech. 248, 567–581 (1993). 33 R. D. Zucker and O. Biblarz, Fundamentals of Gas Dynamics (John Wiley & Sons, New Jersey, 2002).
- [14] 15 H. D. Kim and J. S. Lee, "An experimental study of supersonic ejector for a vacuum pump," in Proceedings of The Korean Society of Mechanical Engineers, Annual Fall Meeting (Korean Society of Mechanical Engineering, Seoul, Republic of Korea, 1994), Vol. B, pp. 520–525.
- [15] 16 J.C.Dutton, C.D.Mikkelsen, and A.L.Addy, "A theoretical and experimental investigation of the constant area supersonic- supersonic ejector," AIAA J. 20(10), 1392–1400 (1982).
- [16] 17 J. Fabri and J. Paulon, "Theory and experiment on supersonic air-to-air ejectors," NACA Technical Memorandum 1410, 1958.
- [17] 18 J. H. Keenan and E. P. Neumann, "A simple air ejector," Trans. ASME: J. Appl. Mech. 64, 75–81 (1942).
- [18] 19 J. H. Keenan, E. P. Neumann, and F. Lustwerk, "An investigation of ejector design by analysis and experiment," Trans. ASME: J. Appl. Mech. 72, 299–309 (1950).
- [19] 20 J. M. Abdulateef, K. Sopian, M. A. Alghoul, and M. Y. Sulaiman, "Review on solar-driven ejector refrigeration technologies," Renewable Sustainable Energy Rev. 13, 1338–1349 (2009).
- [20] 21 K. Annamalai, K. Visvanathan, V. Sriramulu, and K. A. Bhaskaran, "Evaluation of the performance of supersonic exhaust diffuser using scaled down models," Exp. Therm. Fluid Sci. 17, 217–229 (1998).
- [21] 22 K. Chunnanond and S. Aphornratana, "Ejectors: Applications in refrigeration technology," Renewable Sustainable Energy Rev. 8, 129–155 (2004).
- [22] 23 K. K. Ahuja, "Mixing enhancement and jet noise reduction through tabs plus ejectors," AIAA Paper No. 93-4347, 1993.